*Astronomy & Astrophysics* manuscript no. output
November 12, 2026
©ESO 2026

# Euclid First Data Release 1 (DR1)

## Data release overview

Euclid Collaboration: H. Aussel[1]⋆ et al.

[1] Université Paris-Saclay, Université Paris Cité, CEA, CNRS, AIM, 91191 Gif-sur-Yvette, France

November 12, 2026

**ABSTRACT**

This paper describes the contents of the Euclid First Data Release (DR1), together with the set of papers that document the data-processing and the data products. DR1 consists of two parts: first 'DR1-Foundation', releasing images, spectra, and catalogues in November 2026. Second, the shear measurements and the 'Level 3' products required for cosmological analyses will be added in June 2027 to complete the full DR1. This data set contains around a billion catalogued objects, mainly from the Euclid Wide Survey (1975 deg$^2$) and the Euclid Deep Fields (77 deg$^2$).

**Key words.** space vehicles: instruments – surveys – techniques: imaging spectroscopy – techniques: photometric – methods: data analysis

## 1. Introduction

*Euclid* is a space mission of the European Space Agency (ESA) with contributions from the National Aeronautics and Space Administration, with the primary goal of studying dark matter and dark energy using two main probes, weak gravitational lensing and galaxy clustering (Laureijs et al. 2011). *Euclid*'s 1.2-m primary mirror has a field of view (FoV) of 0.54 deg$^2$, with the optics designed to conduct the Euclid Wide Survey (EWS), covering 14 000 deg$^2$ of the extragalactic sky (Euclid Collaboration: Scaramella et al. 2022), along with the smaller and deeper Euclid Deep Survey (EDS). *Euclid* contains two instruments, the VISible instrument (VIS) and the Near-Infrared Spectrometer and Photometer (NISP), which are described in Euclid Collaboration: Cropper et al. (2025) and Euclid Collaboration: Jahnke et al. (2025), respectively. VIS is a broad-band optical imager with a spatial resolution of 0.″18 in the $I_E$ band, while NISP combines the capabilities of an imager in the near-infrared (NIR) bands $Y_E$, $J_E$, and $H_E$ (Euclid Collaboration: Schirmer et al. 2022) with a near-infrared slitless spectrograph (Euclid Collaboration: Gillard et al. 2026). Further details of the *Euclid* mission can be found in the earlier overviews Euclid Collaboration: Mellier et al. (2025) and Euclid Collaboration: Aussel et al. (2026), and the more technical papers referred to in them. Since much of the content of these papers are also relevant to DR1, here we concentrate on the details that differ for this new release.

Although conceived as a cosmology mission, *Euclid*'s wide FoV and deep imaging capabilities in the optical and NIR, along with the complementary ground-based imaging, make its data set useful for studying a wide range of astrophysical topics, as evidenced by the large number of publications that have already appeared. The first data release from *Euclid* was the Early Release Observations (ERO) programme (Cuillandre et al. 2025), highlighting just 24 hours of early data. This was followed by the first 'quick' data release, Q1 (Euclid Collaboration: Aussel et al. 2026), containing the EDS fields at the depth of the EWS, and then Q2 (Beaulieu et al. 2026), a survey of the Galactic bulge.

We present here an overview of the first of the major planned data releases from *Euclid*, the First Data Release (DR1). The initial part of DR1, known as DR1-Foundation (Euclid Data Release 1 2026), contains imaging, spectroscopy, and catalogues from a collection of fields of varying depths covering more than 2000 deg$^2$. The full set of DR1 products, including weak lensing and 3-dimensional galaxy catalogues, together with correlation functions and cosmological analyses from these same areas of the sky will follow in June 2027. In Sect. 2, we present the definition of DR1-Foundation with respect to the full DR1. In Sect. 3, we summarise the data processing and the available data products and in Sect. 4, we give abbreviated descriptions of the other papers supporting DR1.

## 2. The DR1-Foundation data release

The *Euclid* mission will deliver three major data releases, the first one corresponding to approximately the first year of the *Euclid* survey (DR1), the second to the first three years of the survey (DR2), and finally the complete survey (DR3). Here we describe what is contained in DR1-Foundation in the context of DR1. The DR1 content is defined in Pettorino & Ferruit (2026). We review here the main points of this memorandum, which is necessary since DR1 is not limited to the areas of the main *Euclid* surveys, but includes several other regions of the sky.

The *Euclid* survey did not start directly after the satellite's launch, so there were earlier periods, including what is known as the performance-verification (PV) phase, as well as the phase-diversity calibration (PDC) campaign. DR1 also contains calibration observations obtained during or before the routine survey phase, together with science observations that were obtained outside the survey. We briefly describe the timeline of the mission below.

⋆ e-mail: herve.aussel@cea.fr

### 2.1. The phases of the Euclid mission

The *Euclid* mission so far can be split into four phases: (1) launch and commissioning; (2) PV; and (3) the PDC campaign; and (4) the *Euclid* survey. These are described in detail in Euclid Collaboration: Tereno et al. (2026), and we review them briefly here.

*Euclid* was launched on 1 July 2023, and travelled to its nominal halo orbit around the Earth-Sun second Lagrange point (L2) during the month of July (see figure 1 of Euclid Collaboration: Schirmer et al. 2026b, for details). During this time, the spacecraft was thermally decontaminated, the platform and instruments were switched on, and commissioning ran until 31 July.

PV was scheduled for 60 days, beginning on 1 August 2023. Due to insufficient tracking stability of the Fine Guidance Sensor (FGS), it was interrupted several times, including replanning of the PV to advance observations with lower demands on tracking stability; these observations were interleaved with pointing-stability tests. The FGS was successfully recommissioned during 23–30 September 2023, including visits of the self-calibration field, the ERO (Cuillandre et al. 2025), and a dust-obscured area in the Orion Molecular Cloud that was released with the First Quick Data Release (Q1; Euclid Collaboration: Aussel et al. 2026). PV transitioned around 1 December 2023 into the PDC campaign to characterise *Euclid*'s wavefront. The observations of stellar calibration fields – using intrafocal, focal, and extrafocal settings – were separated by approximately 7 days during which the satellite pointing was constrained in order to maintain high thermal stability. Details about the calibration and survey-related aspects of PV and PDC are given in Euclid Collaboration: Schirmer et al. (2026a) and Euclid Collaboration: Tereno et al. (2026).

The *Euclid* survey proper started on 14 February 2024. It consists of observations of the EWS, the EDS, and the Euclid Auxiliary Fields (EAFs), interleaved with various on- and off-sky calibration observations. The last observation of the nominal survey is currently scheduled for 2 January 2030.

Ice contamination in the instrument cavity led to a gradual throughput loss for the VIS instrument, compromising the mission objectives. The first decontamination procedure on 14 March 2024 fully restored the throughput, which then began to rapidly decline at an accelerating rate until 8 June 2024, when *Euclid* was decontaminated once more. This 'ice age' is discussed in sections 5 and 6 of Euclid Collaboration: Schirmer et al. (2026b). The VIS throughput has been remarkably stable since, gradually decreasing by 1–1.5% over the following 2.5 years. The NISP detectors accumulate ice, leading to a slow wavelength-dependent evolution of sensitivity that is well captured by calibrations, but in DR1 not yet corrected for the blue-grism data.

### 2.2. DR1 definition

DR1 is defined loosely as the observations that were obtained since launch, up to the end of the first year of the EWS. To be included, these observations must be 'complete' and 'valid'. 'Complete' means that, in the case of the *Euclid* survey, the ancillary ground-based data (referred to as 'EXT') needed for the scientific exploitation of the observations must be available to the Science Ground Segment (SGS). 'Valid' means that the data quality meets a series of technical requirements. Exposures can be invalidated by external and internal factors, such as solar radiation storms, or guiding and instrument errors. The validity flags set by the instrument processing functions and initial data-merging steps are explained in the articles describing the processing function (PF; see below). The spacecraft's technical reliability is very high, with more than 99% of all pre-planned scientific and telemetry files retrieved on ground (see section 2 in Euclid Collaboration: Schirmer et al. 2026b).

The ice age occupied around three months early in the EWS. This period was excluded from DR1 because of considerable uncertainties in the photometric and point-spread function (PSF) calibration of the VIS data. DR1 corresponds to approximately 12 months of survey observations outside the ice age, concluded by the last observations of the self-calibration block around 2025-05-21T19:12:00Z.

**Table 1.** Definition of DR1 data sets.

| Data set | Definition |
|---|---|
| EWS | CALBLOCK-F-006 |
| EDS | CALBLOCK-F-002 and CALBLOCK-F-003 |
| EAFs | CALBLOCK-F-004, CALBLOCK-F-005 and PV Observation ID 65879 |
| SelfCal | CALBLOCK-F-001 except Patch ID 91[a] and PV Observation IDs 65765, 65776, 65803, 65811 |
| PSF | CALBLOCK-F-008 except Patch ID 158[a] |
| F-010 | CALBLOCK-F-010 |
| F-014 | CALBLOCK-F-014 |
| ILS | Observation IDs 65914 to 66048 (135 Obs. IDs) |
| WAVES | Observation IDs 66059 to 66190 (132 Obs. IDs) |
| SSO | Observation IDs 66202 to 66350 (149 Obs. IDs) |
| EMDS-1 | Observation IDs 66358 to 66491 (134 Obs. IDs) |
| EMDS-2 | Observation IDs 66517 to 66660 (129 Obs. IDs) |
| EMDS-3 | Observation IDs 66680 to 66819 (136 Obs. IDs) |
| EMDS-4 | Observation IDs 66826 to 66962 (136 Obs. IDs) |
| EMDS | Combination of EMDS-1 to EMDS-4 |
| Other | All other CALBLOCKs |

**Notes.** [(a)] These patches were lost to high solar activity. See Sect. 2.3 for brief descriptions of these data sets.

### 2.3. Data-set definitions

The data released in DR1 is not a single homogeneous data set. The raw frames, or Level 1 (LE1) products,[1] for all valid and complete observations are distributed through the Science Archive System (SAS),[2] comprising both calibration and survey observations. However, some of the calibration observations do not produce SGS products. Similarly, not all observations are processed in the same way. For example, individual visits to the Euclid Deep Fields (EDFs) will be processed as EWS observations, but they will also be co-added to produce deep data sets.

Activities performed during an observation are defined by their 'ObservationType', whose name is either CALBLOCK-PV-XXX for the PV phase or CALBLOCK-F-XXX for the routine phase (see Euclid Collaboration: Schirmer et al. 2026a, for a full list). Observations are identified by their Observation ID. If they are, for example, part of the Reference Observation Sequence (ROS; Euclid Collaboration: Tereno et al. 2026) executed at every survey field, then they all share the same Observation ID. Groups of survey fields taken contiguously in time and

[1] See section 7.3.1 of Laureijs et al. (2011) for the definition of the levels in the *Euclid* data processing system.
[2] The entry point is the Euclid Data Space: https://euclid.dataspace.esa.int

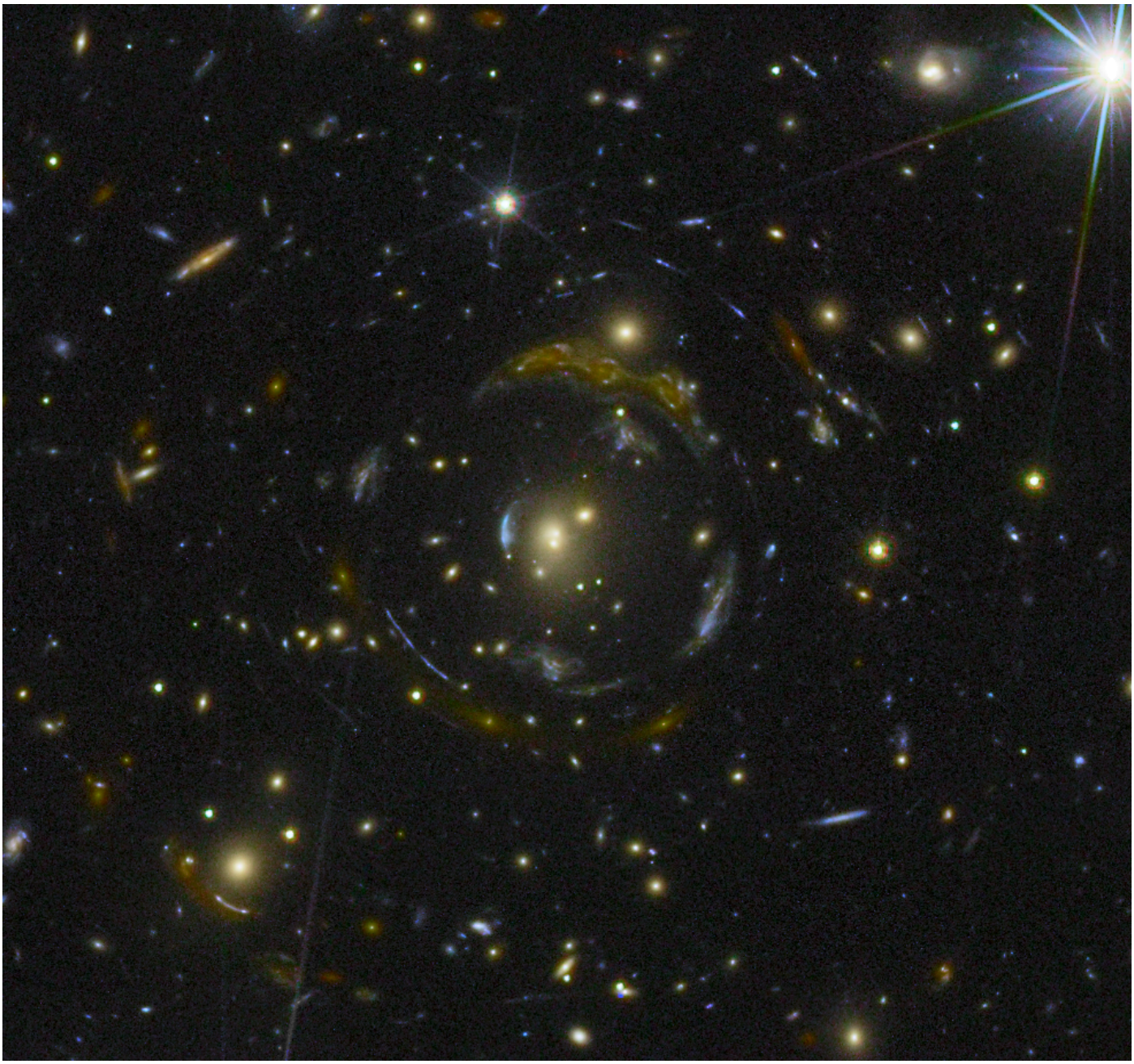


**Fig. 1.** The Carousel Lens at redshift $z = 0.49$, built from DR1 EWS data. The image is $1\farcm5 \times 1\farcm4$ across, with north up and east to the left. Strong lensing has been one of the science highlights coming from DR1-Foundation.

on sky form a 'survey patch', and share its Patch ID. These labels and identifiers uniquely identify the content of DR1 (Table 1).

The sky content of DR1 is presented in Euclid Collaboration: Tereno et al. (2026). The largest constituents are two irregularly shaped blocks, EWS-South and EWS-North, covering approximately 1600 deg$^2$ and 500 deg$^2$, respectively. The EDS fields have gained considerable depth since their first release in Q1 (Euclid Collaboration: Aussel et al. 2026): The EDF-N, EDF-S, and EDF-F were visited 11, 10, and 2 times, respectively, each visit (or 'pass') having the same depth as a single EWS field. The red grism was used throughout, apart from three passes of the EDF-N, for which the ROS was configured with the blue grism. The final effective exposure-time ratio is set to around 25:15 (blue:red) visits, adjusted for zodiacal background brightness.

The Euclid Medium-Deep Survey (EMDS) is around 1 mag deeper and one order of magnitude smaller than the EWS, and consists of the four sub-surveys EMDS-1 to EMDS-4. The EMDS-1 and EMDS-2 parts were taken during the PDC thermal stabilisation periods, which required NISP in idling mode to maximise thermal stability; only VIS data are available for these. The EMDS is part of DR1-Foundation.

The EAFs consist of well-known extragalactic fields used for calibration of photometric redshifts, and to assess the effect of colour gradients within galaxies on shear measurements in the presence of a chromatic PSF. (Euclid Collaboration: Hartley et al. 2026). For DR1, these are the Cosmic Evolution Survey (COSMOS; Scoville et al. 2007), Chandra Deep Field South (CDFS; Giacconi et al. 2002), and All-Wavelength Extended

Groth Strip International Survey (AEGIS; Davis et al. 2007) fields. Others will be observed later during the survey.

The self-calibration (or 'SelfCal') field covers around 2.0 deg$^2$ near the north ecliptic pole (NEP), within *Euclid*'s continuous viewing zone, and is within the area of the EDF-N. Data were acquired through CALBLOCK-F-001 and CALBLOCK-PV-001, covering the full area. More data have been acquired through CALBLOCK-F-014, which executes the ROS at the centre of the self-calibration field for throughput monitoring during PDC and after a thermal decontamination of the spacecraft. Together, these data comprise the extremely deep Euclid Ultra-Deep Field (EUDF), which will be released early in 2027 (McCracken et al., in prep.).

Several PSF-calibration fields (CALBLOCK-F-008) are also part of DR1. They are observed every 2–6 weeks to obtain representative PSF measurements for every survey patch. A special pattern of 100 dithers is used, at each of which VIS takes a 289-s exposure. During this time, NISP takes off-sky nonlinearity calibrations. PSF-calibration fields are observed at least once also with one ROS equivalent, to secure NISP data for stellar classification.

The 'ILS' fields were defined by the Independent Legacy Scientists (ILSs) and 'WAVES' is part of the Wide-Area VISTA Extragalactic Survey (Driver et al. 2019). Lastly, 'SSO' is a survey field designed for Solar System objects, close to the ecliptic plane. These three components are described in more depth in Euclid Collaboration: Tereno et al. (2026).

### 2.4. DR1-Foundation

All DR1 data were reprocessed with the SGS processing function in its frozen DR1 configuration, ensuring maximum homogeneity (Sect. 3). Reprocessing started in May 2025 for the EXTernal data (EXT; Euclid Collaboration: Corcho-Caballero et al. 2026). On the spectroscopic side, the Level 2 (LE2) processing was completed at the end of September 2025. On the imaging side, the LE2 products up to PHZ were available mid-September 2025, but it took until the end of October 2025 to produce the SHEar measurements (SHE) PSF model and shape measurements. The full reprocessing timeline is given in figure 8 of Euclid Collaboration: Ruffenach et al. (2026).

Once the products have been computed, they undergo a series of tests by the relevant Organisation Unit (OU) to check whether they are compliant with the mission's scientific requirements. This validation can take up to 1–2 months in the case of more complex products. In early 2026, it became evident that the PSF model underestimated the size of the VIS PSF and would thus compromise the shear analysis.

With SHE processing requiring at least 2 months, this would have left less than 6 months for a full cosmological analysis before the nominal release date of 12 November 2026. Since all other LE2 products had been internally released a year before this date, a staggered approach was decided for the public release. DR1-Foundation occurs on 12 November 2026, including LE1 and validated LE2 data products, such as images, spectra, and catalogues. The LE3 data products, comprising shape measurements, weak lensing (WL) and galaxy clustering (GC) correlation functions, and the cosmological analyses, are added in June 2027. Together, they form the full DR1; the data products that comprise DR1-Foundation will not be re-released in June 2027.

## 3. Data processing and data products

The *Euclid* mission data are processed by the Euclid Consortium (EC) SGS. Euclid Collaboration: Ruffenach et al. (2026) describes the architecture of this distributed computing system, together with account of the DR1 data processing. They provide in their figure 3 an overview of the pipeline with the PF and their main products, and the connection between them. This figure has been updated in Fig. 2 here to reflect the processing chain and data products distributed as part of DR1-Foundation. This processing chain is very similar to the one executed for the Q1 data release (Euclid Collaboration: Aussel et al. 2026), but each PF has been substantially improved to produce DR1-Foundation; this is demonstrated in Fig. 1,[3] showing the Carousel Lens system (Huang et al. 2021; O'Donnell et al. 2022). We now briefly review these improvements and indicate the relevant papers where complete information can be obtained.

### 3.1. Telemetry decommutation and LE1 products

The LE1 processing is identical to that performed for Q1 and described in Euclid Collaboration: Aussel et al. (2026). The LE1 PF produces the VIS raw-frame product, the NISP raw-frame product, and the housekeeping and telemetry (HKTM) product from the telemetry received from the Mission Operation Centre (MOC). These are described in detail in the Data Product Description Document (DPDD).[4] Only VIS and NISP raw frames are distributed with DR1-Foundation. The HKTM products are used by the SHE PF to reconstruct the pointing history during an exposure and will de distributed at the time of the full DR1.

The scheduled observations column of Table 2 allows us to estimate the reliability of the *Euclid* mission observations. In the EWS, for VIS, 17 143 nominal exposures were collected from 19 588 scheduled in the Reference Survey Definition (RSD), or about 87%, within the mission requirements. Missing data or failures are due to, for example, invalid data products or missing ground-based EXT coverage data. This last point is a factor that limited PSF calibration for the DR1 processing, because stellar spectral energy distributions (SEDs) were not yet completely available. We expect higher completion rates for DR2 and DR3.

### 3.2. VIS data processing

The VIS instrument data are processed by the VIS PF. The processing is described in Euclid Collaboration: McCracken et al. (2026b). Numerous tasks, such as cosmic-ray rejection, photometric calibration, background estimation, coaddition, and the content of the delivered data products were improved for DR1. These updates, together with a comprehensive assessment of data quality and an outlook for further improvements, are described in Euclid Collaboration: McCracken et al. (2026a).

The number of validated LE2 exposures – with the nominal integration time of 565 s, or the 289 s exposure time for the PSF data set – are reported in Table 3 for each data set, together with their covered areas. Their distribution on the sky is shown in Fig. 3.

### 3.3. NIR data processing

NISP calibrated frames are processed by the NIR PF (Euclid Collaboration: Polenta et al. 2026b). Substantial improvements

[3] Image built with `http://pypi.org/project/eummy/`
[4] `https://euclid.esac.esa.int/dr/dr1/dpdd`

**Table 2.** LE1 Data products released as part of DR1-Foundation, listing the number of LE1 products of each type for each data set.

| | Scheduled | VIS raw frames | | NISP raw frames | | | |
|---|---|---|---|---|---|---|---|
| Data set | observations | VIS nominal | VIS short | NISP spectro | NISP $Y_E$ | NISP $J_E$ | NISP $H_E$ |
| EWS | 19588 | 17143 | 8572 | 17231 | 17231 | 17231 | 17231 |
| EDFs | 4568 | 4339 | 2170 | 4392 | 4392 | 4392 | 4392 |
| EAFs | 896 | 896 | 358 | 896 | 896 | 896 | 896 |
| SelfCal | 1216 | 1140 | 30 | 1140 | 1140 | 1139 | 1139 |
| PSF | 2136 | 1964 | 0 | 0 | 1648 | 0 | 0 |
| F014 | 104 | 88 | 32 | 89 | 88 | 88 | 88 |
| F010 | 856 | 819 | 22 | 856 | 16 | 16 | 16 |
| ILS | 540 | 536 | 268 | 498 | 498 | 498 | 498 |
| WAVES | 528 | 520 | 260 | 44 | 44 | 44 | 44 |
| SSO | 596 | 596 | 298 | 596 | 596 | 596 | 596 |
| EMDS1 | 536 | 532 | 266 | 0 | 0 | 0 | 0 |
| EMDS2 | 516 | 516 | 258 | 0 | 0 | 0 | 0 |
| EMDS3 | 544 | 455 | 228 | 528 | 528 | 528 | 528 |
| EMDS4 | 544 | 427 | 217 | 528 | 528 | 528 | 528 |
| Total | 48524 | 39274 | 13375 | 30764 | 30221 | 28562 | 28562 |
| Other | | | 9699[a] | 3966 | 2616 | 2606 | 2606 |

**Notes.** See Sect. 2.3 for an explanation of the data set names. [(a)] For the 'Other' category, the distinction between VIS nominal and short exposures has no meaning because calibrations are obtained with many different exposure times.

**Table 3.** Number of VIS and NISP LE2 nominal-exposure validated calibrated frames per data set, and the corresponding areas.

| Data set | No. exposures | Area | No. exposures | | | Area |
|---|---|---|---|---|---|---|
| | $I_E$ | [deg$^2$] | $Y_E$ | $J_E$ | $H_E$ | [deg$^2$] |
| EWS | 16913 | 2092.2 | 16111 | 15787 | 15977 | 1975.4 |
| EDFs | 4568 | 77.0 | 3942 | 3898 | 3930 | 76.8 |
| EDF-N | 2408 | 24.3[a] | 1806 | 1756 | 1799 | 19.8[a] |
| EDF-F | 184 | 13.1[a] | 182 | 181 | 178 | 13.0[a] |
| EDF-S | 1976 | 27.8[a] | 1954 | 1961 | 1957 | 23.2[a] |
| Total | 4568 | 65.2[a] | 3942 | 3898 | 3934 | 56.0[a] |
| EAFs | 895 | 4.8 | 910 | 908 | 907 | 4.8 |
| SelfCal | 1215 | 2.2 | 1972 | 1977 | 1978 | 2.2 |
| PSF | 2130 | 6.3 | 0 | 0 | 0 | 0.0 |
| F010 | 856 | 1.8 | 15 | 15 | 15 | 1.8 |
| F014 | 103 | 1.6 | 57 | 54 | 55 | 1.6 |
| ILS | 538 | 37.5 | 466 | 470 | 471 | 35.9 |
| WAVES | 525 | 14.8 | 0 | 0 | 0 | 0.0 |
| SSO | 593 | 19.2 | 595 | 598 | 587 | 18.2 |
| EMDS-1 | 533 | 15.1 | 0 | 0 | 0 | 0.0 |
| EMDS-2 | 516 | 13.0 | 0 | 0 | 0 | 0.0 |
| EMDS-3 | 536 | 15.9 | 450 | 438 | 442 | 15.7 |
| EMDS-4 | 541 | 13.9 | 396 | 388 | 395 | 12.2 |
| Total | 33135 | 2268.7 | 24068 | 23681 | 23910 | 2268.7 |

**Notes.** [(a)] For the EDFs this corresponds to the deep area with maximum overlap.

were implemented for DR1 (Euclid Collaboration: Polenta et al. 2026a), in particular with an updated in-flight calibration plan that allows for better persistence masking. Persistence in the NISP detector is discussed in Euclid Collaboration: Kubik et al. (2026), where a model predicting the amount of signal is described.

Table 3 also gives the number of validated calibrated NIR frames in each NISP photometric bands delivered in DR1-Foundation. The corresponding area where all three bands are valid is indicated in the last column.

The astrometric calibration of NIR frames is described in Euclid Collaboration: Radovich et al. (2026). While most of the data are within requirements, a fraction (0.7%) of the DR1 area has error larger than 50 mas. A `HEALPix` information map of the astrometric error is provided by the Visibility Mask PhotoZ (VMPZ-ID) PF (Euclid Collaboration: Odier et al. 2026).

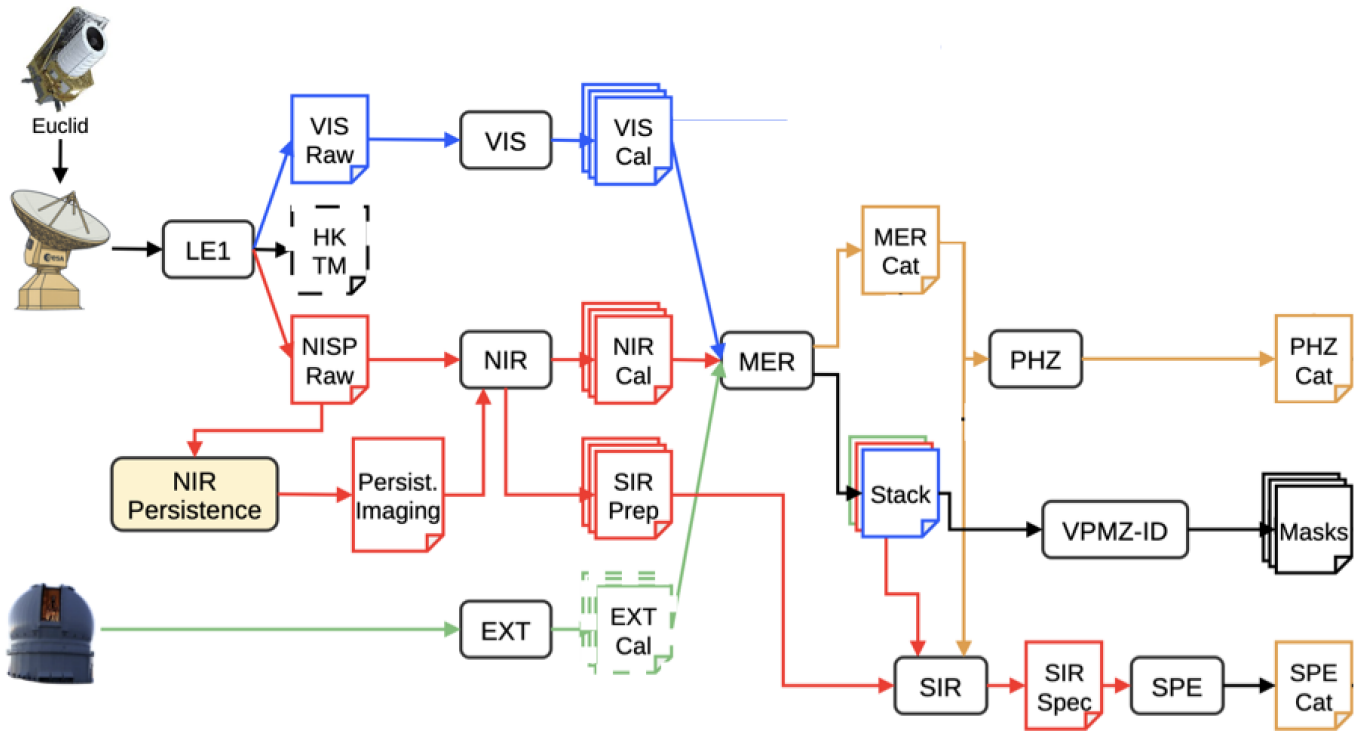



**Fig. 2.** Overview of DR1 data processing, showing the main data products making up the DR1 data release, together with the SGS PF creating them, and outlining the flow of the various data sets. 'Raw' products refer to products created from the decommuted telemetry without any further processing. 'Cal' products refer to calibrated data, with instrument signatures being removed and data put on a physical scale. 'Stack' refers to image combinations, 'Spec' to combined 1D spectra, and 'Cat' to catalogues. This is an adapted figure 3 from Euclid Collaboration: Ruffenach et al. (2026) to show the process for DR1-Foundation only. Products indicated with a dashed outline are created and used in the pipeline, but are not distributed as part of DR1-Foundation.

Finally, the NIR PSF is modelled by Euclid Collaboration: da Silva et al. (2026).

### 3.4. EXT processing

*Euclid* is said to have a third instrument besides VIS and NISP: this is because of the EXT data, which provide the homogeneous ground-based imaging needed to derive the photometric redshifts and SEDs of the objects detected in MER. We use as input a series of large surveys. For the EWS, the northern data are provided by Ultraviolet Near-Infrared Optical Northern Survey (UNIONS) and the southern data by Dark Energy Survey (DES), as described in Gwyn et al. (2025) and Abbott et al. (2021), respectively. Euclid Collaboration: Corcho-Caballero et al. (2026) details how these data are ingested in the SGS, how they are recalibrated, and how their quality is assessed.

While the EXT processing is improved with respect to Q1, a few issues are still present in the DR1 EXT products, as discussed in section 6 of Euclid Collaboration: Corcho-Caballero et al. (2026). This is especially the case with the Panchromatic Survey Telescope and Rapid Response System (Pan-STARRS) imaging (Chambers et al. 2016), where an incorrect handling of the flags by the SGS has led to areas with degraded photometry. In the same spirit as for the astrometric NIR issue outlined in Sect. 3.3, a dedicated `HEALPix`[5] (Górski et al. 2005) information map is provided in the DR1-Foundation VMPZ-ID products (Euclid Collaboration: Odier et al. 2026). We stress here that this issue arises from our processing, not from the UNIONS data, which are of excellent quality. The EXT pipelines have been updated so that this issue will not be present any more in the DR2 release.

### 3.5. MER data processing

MER is the PF in charge of the creation of *Euclid* data stacks from the individually calibrated exposures delivered by VIS and NIR on a common astrometric grid. It also carried out the detection of objects and measurement of their properties. The DR1 version of the MER PF builds on the version that was used for Q1 (Euclid Collaboration: Romelli et al. 2026), with various improvements such as the computation of a local noise level, and the addition of new quantities in the catalogue. These, together with the extensive validation of the images and catalogues, are presented in Euclid Collaboration: Kümmel et al. (2026).

Euclid Collaboration: Gasparetto et al. (2026) makes use of comparison with the COSMOS2025 catalogue (Shuntov et al. 2025) independently measured on one of the EAFs. This provides an extensive check of the MER photometry, both at the EWS depth and at the greater depth that can be reached on this field.

Note that the MER processing is normally triggered if all the VIS, NIR, and EXT data exist. In some cases, MER has been run when only the VIS and NIR data were present, in order to allow for the spectroscopic processing to run, as it needs the MER catalogue as input. For this reason, DR1-Foundation does not contain MER data for some of the data sets. The type of MER processing per data set is provided in Table 4. 'MER Wide' is the standard processing for each ROS, while 'MER Deep' com-

[5] `https://healpix.sourceforge.io`

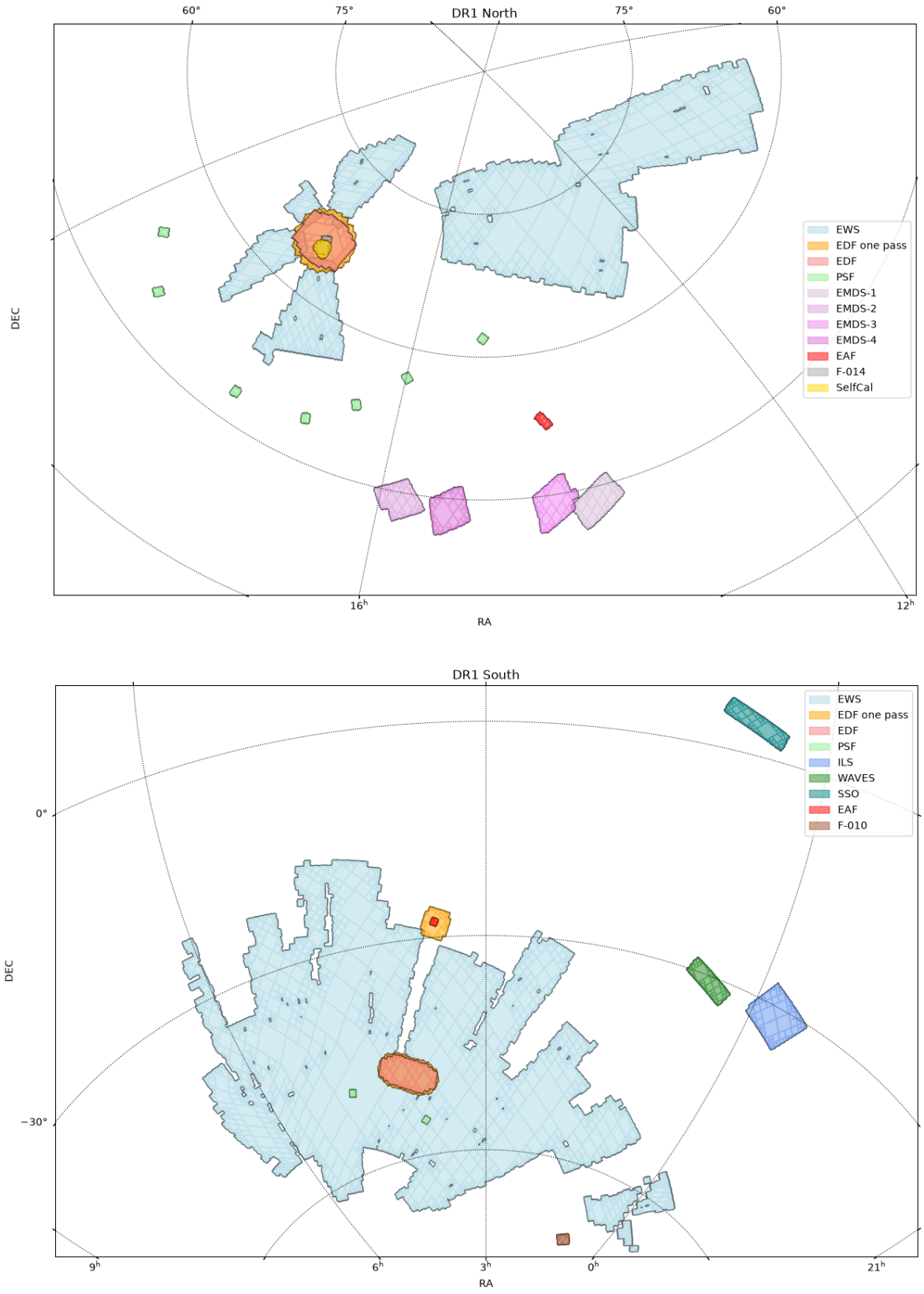



**Fig. 3.** Distribution on the sky of the various DR1 data sets in the north (top) and in the south (bottom). Note that there are no EWS data underneath the EDF-N. In the south, there are no EWS data in the EDF-F, but the area of the EDF-S has been observed as part of the EWS. In the north, the EAF area is AEGIS, while in the south, it is the CDFS in the centre of the EDF-F. The third EAF, COSMOS, is outside the field of view of these figures.

**Table 4.** Types of MER processing available per data set.

| Data set | MER Processing |
|---|---|
| EWS | MER Wide |
| EDFs | MER Deep + Wide |
| EAF–COSMOS | MER Deep + Wide |
| EAF–CDFS | MER Deep + Wide |
| EAF–AEGIS | MER VIS + NIR |
| SelfCal | MER Wide |
| PSF | ... |
| F010 | MER VIS + NIR |
| F014 | MER Wide |
| ILS | MER VIS + NIR |
| WAVES | ... |
| SSO | MER VIS + NIR |
| EMDS-1 | ... |
| EMDS-2 | ... |
| EMDS-3 | MER VIS + NIR |
| EMDS-4 | MER VIS + NIR |

bines all ROSs available for depth. 'MER VIS + NIR' means that MER was triggered even if no EXT data are available, in order to be able to run the SIR pipeline. Note that in this table we break the EAF data set into its three separate fields, since we did not have EXT processing of the ground-based data for AEGIS.

### 3.6. PHZ data processing

The PHZ PF provides the photometric redshifts and physical properties of the sources in the MER catalogue. The Q1 version of the PF is described in Euclid Collaboration: Tucci et al. (2026). For DR1, the main addition is the availability of EAFs to calibrate the `NNPZ` (see Euclid Collaboration: Enia et al. 2024) reference sample so that the object redshift probability distributions can be derived using this package (Euclid Collaboration: Hartley et al. 2026). Improvements have also been made for the computation of the physical properties of sources, as described in Euclid Collaboration: Enia et al. (2026). Overall, DR1-Foundation provides photometric redshifts and classification for 880 million sources over the 1900 deg$^2$ of the EWS.

### 3.7. VMPZ-ID data processing

The VMPZ-ID is formally a Level 3 (LE3) processing function, whose purpose is to determine the selection function and create random catalogues of the imaging part of the EWS. However, in order to compute these final products, it also assembles information about the data drawn directly from LE2 products. Some of these products are very useful for the scientific exploitation of the DR1-Foundation data set, and are close enough to their LE2 origin that they have been included in this release. All these products are either masks or maps of useful quantities distributed as `HEALPix` maps. The construction of these numerous products is described in Euclid Collaboration: Odier et al. (2026). The VMPZ-ID PF was only run on the EWS and EDF data sets.

### 3.8. SIR and SPE data processing

The processing of the spectroscopic exposures is carried out in two PFs. First, the spectra are extracted by the Spectroscopy InfraRed (SIR) PF. The processing is described by Euclid Collaboration: Copin et al. (2026), with numerous improvements such as better persistence flagging and a more efficient extraction algorithm (Euclid Collaboration: Scodeggio et al. 2026). This was made possible by the accurate calibration of the instrument, with the spectral curvature, dispersion solution, PSF as a function of wavelength, and other parameters being accounted for (Euclid Collaboration: Fumana et al. 2026). As a result, a spectrum has been extracted in DR1 for all objects in the MER catalogue with $H_E < 23.5$; this is a full magnitude deeper than what was done for Q1.

The spectra are then passed to the SPE PF for redshift estimation, spectral classification, and spectral feature measurements. The DR1 version of the PF builds on the one used for Q1 (Euclid Collaboration: Le Brun et al. 2026b), with improved templates and better measurement methods (Euclid Collaboration: Le Brun et al. 2026a). The SPE PF also benefits from the higher quality of the spectra delivered by SIR. As a result, a comparison with Dark Energy Spectroscopic Instrument (DESI) redshifts (DESI Collaboration et al. 2024) finds good agreement, with a scatter half that of the Q1 sample. Finally, the DR1-Foundation data set contains observations of the EDF-N with both the blue and red grisms, allowing us to obtain a high purity sample that will be used to derive the spectroscopic selection function for the full DR1 data release.

As for Q1, because of the nature of the measurement where we extract a spectrum for all objects with $H_E < 23.5$, we caution the users of the DR1-Foundation release against blindly using the redshifts: many spectra do not show any measurable features, yet have an entry in the SPE catalogue. Euclid Collaboration: Le Brun et al. (2026a) discusses redshift reliability and the flags that can be used to assess this.

### 3.9. Data volume

The volume of data being made available in DR1-Foundation corresponds to approximately 1.7 PB (Euclid Collaboration: Ruffenach et al. 2026). Included are more than 120 000 calibrated frames from VIS and NISP. There are also uniformly reduced and calibrated EXT data, primarily from UNIONS in EWS-North and DES in the EWS-South, and other imaging data in the EDFs and EAFs.

Dr1-Foundation also contains over 170 million validated spectra in both red- and blue-grism modes extracted from the NISP dispersed images, most having spectroscopic redshift estimates. Over 60 million sources are identified as quasar candidates from photometric data.

There are more than a billion catalogued sources in DR1. Focussing on those sources categorised as galaxies (specifically with `PHZ_CLASSIFICATION=2`), the total number of over 900 million breaks down as follows:

- EWS, 817 846 065;
- EDS, 49 393 051;
- EAFs, 34 427 023.

## 4. Technical papers associated with DR1

DR1-Foundation is documented by a comprehensive list of papers (Table 5) that provide the necessary context for its scientific exploitation. These papers are published along with this overview paper, discussing the updates made with respect to Q1, the currently known limitations of DR1, and upcoming improvements for DR2.

Euclid Collaboration: Tereno et al. (2026) details the multiple *Euclid* surveys and fields, including the EDS, EAFs, calibration fields, EMDS, the Euclid Ecliptic Survey, and the ILS field, in addition to the EWS. It also describes the Science Operations Centre (SOC) activities of the operational sky survey (OSS) generation and the production of operational products.

Euclid Collaboration: Ruffenach et al. (2026) describes the operation and architecture of the *Euclid* SGS, covering the role of the SOC, the Science Data Centres (SDCs), and the SGS common infrastructure, including the Euclid Archive System (EAS). It also discusses the processing methodology and daily processing operations. The production of Euclid DR1 involved the execution of 35 million processing jobs and 6.7 million core hours of computing.

Euclid Collaboration: McCracken et al. (2026a) describes the VIS DR1 data set totalling 42 092 images, evaluates the performance of the VIS processing function pipeline and discusses the global properties of the processed VIS images. In particular the levels of astrometric and photometric precision are quantified and shown to be within mission requirements.

Euclid Collaboration: Polenta et al. (2026a) describes the near-infrared processing function (NIR), covering its processing algorithms, calibration, data products, and validation. NISP astrometric and photometric precision are also shown to be within requirements. In total, the DR1 processing produced 80 695 calibrated frames of NISP data.

Euclid Collaboration: Radovich et al. (2026) provides further details of the NISP astrometry, describing how instrumental distortions are modelled and corrected, with comparison to stellar positions from *Gaia* (Gaia Collaboration: Vallenari et al. 2023).

Euclid Collaboration: da Silva et al. (2026) describes the modelling of the NISP PSF, part of the NIR processing function, investigating how this varies with time, focal-plane position, and wavelength.

Euclid Collaboration: Fumana et al. (2026) describes the spectroscopic calibration carried out by the spectroscopic SIR processing function. This provides validated spectra for more than 170 million sources.

Euclid Collaboration: Kubik et al. (2026) describes the effects of detector persistence in the NISP instrument, including the masking strategy used in DR1.

Euclid Collaboration: Corcho-Caballero et al. (2026) gives a detailed description of the processing and calibration steps applied to the ground-based optical imaging data sets (EXT) released in DR1. In particular, there is a description of how stacked data products are generated and an assessment of the EXT data quality.

Euclid Collaboration: Kümmel et al. (2026) describes the MERge processing function, which detects objects in the VIS, NISP, and EXT imaging data, measures their properties, and combines them into a single multi-wavelength catalogue.

Euclid Collaboration: Gasparetto et al. (2026) describes the use of existing data from the COSMOS field (Shuntov et al. 2025) to validate the DR1 photometry.

Euclid Collaboration: Hartley et al. (2026) describes the photometric redshift processing function (PHZ), which also provides spectral energy distribution fits for galaxies and stars.

Euclid Collaboration: Enia et al. (2026) supplements the other PHZ paper by presenting the estimation of galaxy physical parameters for non-cosmological science, in particular studying the relationship between stellar mass and star-formation rate.

Euclid Collaboration: Le Brun et al. (2026a) describes the spectroscopic SPE processing function, which analyses the 1-dimensional spectra from NISP It also carries out spectroscopic classification, redshift determination, and the measurement of spectral features.

Euclid Collaboration: Odier et al. (2026) describes the series of photometric masks developed by the VMPZ-ID processing function for use with the DR1 data. This includes the effective coverage mask, as well as specific masks representing spatial variations of various properties of the observations.

Euclid Collaboration: Schirmer et al. (2026a) describes the overall calibration strategy, the performance of the calibration plan with respect to top-level mission calibration requirements, and current short-comings, as well as planned improvements.

Euclid Collaboration: Schirmer et al. (2026b) assesses the spacecraft performance in the L2 environment up until October 2026, covering – among other issues – stray-light sensitivity, thermo-optical properties, molecular contamination, tracking stability, and meteoroid impacts.

Additional papers are still in preparation (Table 5). A complete set will appear in support of the full DR1 in June 2027.

## 5. Conclusions

Covering around 2000 deg$^2$, the publicly available Euclid DR1-Foundation is, to date, the largest sky area observed from space at optical and near-infrared wavelengths. The sub-arcsecond resolution imaging is complemented by slitless spectroscopy. These high-quality data have begun to help answer a vast number of scientific questions – some of which had never been conceived of when *Euclid* was designed – and enable numerous new discoveries.

Compared with earlier modest releases, science exploitation for DR1-Foundation is proceeding differently, now that the data sets are so extensive. The Q1 data release was accompanied by a large number of papers presenting discoveries based on those data. For DR1-Foundation, such papers will appear when they are ready, some along with DR1-Foundation, others in the very near future, but many more in the coming months. These tackle a wide range of different science cases that can be addressed

**Table 5.** List of papers supporting DR1.

| No. | Title | Authors |
|---|---|---|
| 1 | Data release overview | Aussel et al. |
| 2 | The *Euclid* surveys at DR1 | Tereno et al. |
| 3 | An overview of the Science Ground Segment architecture and operations | Ruffenach et al. |
| 4 | VIS processing and data products | McCracken et al. |
| 5 | Near-infrared processing and data products | Polenta et al. |
| 6 | NIR astrometric calibration | Radovich et al. |
| 7 | NISP-P point-spread function modelling pipelines | da Silva et al. |
| 8 | SIR spectroscopic calibration | Fumana et al. |
| 9 | Persistence in NISP detectors | Kubik et al. |
| 10 | Colouring *Euclid* with external ground-based imaging data | Corcho-Caballero et al. |
| 11 | The MERge processing | Kümmel et al. |
| 12 | Multi-band photometry validation on COSMOS extragalactic sources | Gasparetto et al. |
| 13 | Photometric redshift pipeline overview and validation | Hartley et al. |
| 14 | The PHZ processing function for the physical properties of galaxies | Enia et al. |
| 15 | Performance of the redshift measurement and spectroscopic analysis | Le Brun et al. |
| 16 | *Euclid* photometric masks | Odier et al. |
| 17 | Calibration strategy and observations | Schirmer et al. |
| 18 | Spacecraft performance in the L2 environment | Schirmer et al. |
| | The SIR spectroscopic processing function | in prep. |
| | Euclid Archive System: data processing system and data storage system | in prep. |
| | The Euclid Data Space | in prep. |
| | *Gaia*-based calibration | in prep. |
| | EXT Dark Energy Survey data reduction | in prep. |
| | EXT PSF modelling pipeline | in prep. |
| | $N(z)$ estimation and calibration performance | in prep. |
| | $N(z)$ estimates validation | in prep. |
| | Shear overview, requirements, methods, and validation | in prep. |
| | Shear Data Catalogue | in prep. |
| | Shear calibration | in prep. |
| | MetaCal | in prep. |
| | *Euclid* VIS PSF model | in prep. |
| | *Euclid* VIS PSF calibration | in prep. |
| | *Euclid* VIS PSF field calibration | in prep. |
| | Thermal property tracking in the image domain | in prep. |
| | Mitigation strategies for the photometric 2-pt correlation function | in prep. |
| | Photometric visibility mask and randoms for the 2-pt correlation function | in prep. |
| | Photometric masks and effective coverage for cluster detection | in prep. |
| | Photometric masks and combined catalogues | in prep. |
| | In-orbit performance of the NISP Instrument | in prep. |

with the DR1-Foundation data, from the search for solar-system objects to the discovery of distant quasars and spectacular strong lenses.

In June 2027, DR1 will be completed with shear measurements, along with weak-lensing and galaxy-clustering correlation functions, thereby beginning to deliver the cosmological science for which *Euclid* was built. We stress that the upcoming full DR1 release will use the DR1-Foundation products. No product released as part of DR1-Foundation will be reprocessed for DR1. DR1 will only add the SHE and numerous LE3 products.

*Euclid* continues to operate smoothly and with extraordinarily high reliability. At the time of writing, *Euclid* has observed approximately 8700 $\deg^2$ of the sky. Together with DR1, these data are being used to continuously improve the pipelines for DR2, scheduled for 2029.

*Acknowledgements.* The Euclid Consortium acknowledges the European Space Agency and a number of agencies and institutes that have supported the development of *Euclid*, in particular the Agenzia Spaziale Italiana, the Austrian Forschungsförderungsgesellschaft funded through BMIMI, the Belgian Science Policy, the Canadian Euclid Consortium, the Deutsches Zentrum für Luft- und Raumfahrt, the DTU Space and the Niels Bohr Institute in Denmark, the French Centre National d'Etudes Spatiales, the Fundação para a Ciência e a Tecnologia, the Hungarian Academy of Sciences, the Ministerio de Ciencia, Innovación y Universidades, the National Aeronautics and Space Administration, the National Astronomical Observatory of Japan, the Netherlandse Onderzoekschool Voor Astronomie, the Norwegian Space Agency, the Research Council of Finland, the Romanian Space Agency, the Swiss Space Office (SSO) at the State Secretariat for Education, Research, and Innovation (SERI), and the United Kingdom Space Agency. A complete and detailed list is available on the *Euclid* web site (www.euclid-ec.org/consortium/community/). This work has made use of the Euclid Data Release 1 (DR1) from the European Space Agency (ESA) mission *Euclid*, available at https://www.cosmos.esa.int/web/euclid/data-release-dr1.

## References

Abbott, T. M. C., Adamów, M., Aguena, M., et al. 2021, ApJS, 255, 20
Beaulieu, J.-P., Bachelet, E., Gilles, M., et al. 2026, A&A, accepted, arXiv:2606.25883

Chambers, K. C., Magnier, E. A., Metcalfe, N., et al. 2016, arXiv e-prints, arXiv:1612.05560
Cuillandre, J.-C., Bertin, E., Bolzonella, M., et al. 2025, A&A, 697, A6
Davis, M., Guhathakurta, P., Konidaris, N. P., et al. 2007, ApJ, 660, L1
DESI Collaboration, Adame, A. G., Aguilar, J., et al. 2024, AJ, 168, 58
Driver, S. P., Liske, J., Davies, L. J. M., et al. 2019, The Messenger, 175, 46
Euclid Collaboration: Aussel, H., Tereno, I., Schirmer, M., et al. 2026, A&A, 711, A1
Euclid Collaboration: Copin, Y., Fumana, M., Mancini, C., et al. 2026, A&A, 711, A6
Euclid Collaboration: Corcho-Caballero, P., Balbinot, E., De Jong, J., et al. 2026, A&A, submitted
Euclid Collaboration: Cropper, M., Al-Bahlawan, A., Amiaux, J., et al. 2025, A&A, 697, A2
Euclid Collaboration: da Silva, R., Faustini, F., Polenta, G., et al. 2026, A&A, submitted
Euclid Collaboration: Enia, A., Bolzonella, M., Pozzetti, L., et al. 2024, A&A, 691, A175
Euclid Collaboration: Enia, A., Hartley, W., Bolzonella, M., et al. 2026, A&A, submitted
Euclid Collaboration: Fumana, M., Copin, Y., Appleton, P., et al. 2026, A&A, submitted
Euclid Collaboration: Gasparetto, T., Merlin, E., Castellano, M., et al. 2026, A&A, submitted
Euclid Collaboration: Gillard, W., Maciaszek, T., Prieto, E., et al. 2026, A&A, 707, A227
Euclid Collaboration: Hartley, W., Paltani, S., Dubath, F., et al. 2026, A&A, submitted
Euclid Collaboration: Jahnke, K., Gillard, W., Schirmer, M., et al. 2025, A&A, 697, A3
Euclid Collaboration: Kubik, B., Conseil, S., Ferriol, S., et al. 2026, A&A, submitted
Euclid Collaboration: Kümmel, M., Caro, F., Dimauro, P., et al. 2026, A&A, submitted
Euclid Collaboration: Le Brun, V., Bethermin, M., Moresco, M., et al. 2026a, A&A, submitted
Euclid Collaboration: Le Brun, V., Bethermin, M., Moresco, M., et al. 2026b, A&A, 711, A7
Euclid Collaboration: McCracken, H., Benson, K., Cropper, M., et al. 2026a, A&A, submitted
Euclid Collaboration: McCracken, H. J., Benson, K., Dolding, C., et al. 2026b, A&A, 711, A2
Euclid Collaboration: Mellier, Y., Abdurro'uf, Acevedo Barroso, J., et al. 2025, A&A, 697, A1
Euclid Collaboration: Odier, J., Macias-Perez, J., Alguero, G., et al. 2026, arXiv, submitted
Euclid Collaboration: Polenta, G., Frailis, M., Alavi, A., et al. 2026a, A&A, submitted
Euclid Collaboration: Polenta, G., Frailis, M., Alavi, A., et al. 2026b, A&A, 711, A3
Euclid Collaboration: Radovich, M., da Silva, R., Polenta, G., et al. 2026, A&A, submitted
Euclid Collaboration: Romelli, E., Kümmel, M., Dole, H., et al. 2026, A&A, 711, A4
Euclid Collaboration: Ruffenach, M., Frailis, M., Zacchei, A., et al. 2026, A&A, submitted
Euclid Collaboration: Scaramella, R., Amiaux, J., Mellier, Y., et al. 2022, A&A, 662, A112
Euclid Collaboration: Schirmer, M., Jahnke, K., Seidel, G., et al. 2022, A&A, 662, A92
Euclid Collaboration: Schirmer, M., Paterson, K., Alavi, A., et al. 2026a, A&A, submitted
Euclid Collaboration: Schirmer, M., Paterson, K., Altieri, B., et al. 2026b, A&A, submitted
Euclid Collaboration: Scodeggio, M., Copin, Y., et al. 2026, in preparation
Euclid Collaboration: Tereno, I., Dinis, J., Dupac, X., et al. 2026, arXiv, submitted
Euclid Collaboration: Tucci, M., Paltani, S., Hartley, W. G., et al. 2026, A&A, 711, A5
Euclid Data Release 1. 2026, https://doi.org/10.57780/esa-d079c51
Gaia Collaboration: Vallenari, A., Brown, A. G. A., Prusti, T., et al. 2023, A&A, 674, A1
Giacconi, R., Zirm, A., Wang, J., et al. 2002, ApJS, 139, 369
Górski, K. M., Hivon, E., Banday, A. J., et al. 2005, ApJ, 622, 759
Gwyn, S., McConnachie, A. W., Cuillandre, J.-C., et al. 2025, AJ, 170, 324
Huang, X., Storfer, C., Gu, A., et al. 2021, ApJ, 909, 27
Laureijs, R., Amiaux, J., Arduini, S., et al. 2011, ESA/SRE(2011)12, arXiv:1110.3193
O'Donnell, J. H., Wilkinson, R. D., Diehl, H. T., et al. 2022, ApJS, 259, 27
Pettorino, V. & Ferruit, P. 2026, Content of the ESA Euclid Data Release 1 (DR1), https://www.cosmos.esa.int/documents/10647/12245842/DR1-memo_250624.pdf/, accessed 2026-11-08
Scoville, N., Aussel, H., Brusa, M., et al. 2007, ApJS, 172, 1
Shuntov, M., Akins, H. B., Paquereau, L., et al. 2025, A&A, 704, A339